.

Citation: *Egypt.Acad.J.Biolog.Sci. (C.Physiology and Molecular biology) Vol. 15(2) pp723-735 (2023)*
DOI: 10.21608/EAJBSC.2023.327190

Egypt. Acad. J. Biolog. Sci., 15(2):723-735 (2023)

Egyptian Academic Journal of Biological Sciences
C. Physiology & Molecular Biology
ISSN 2090-0767
www.eajbsc.journals.ekb.eg

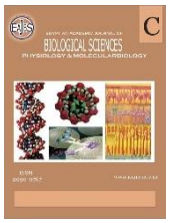

Application and Theoretical Study: New Barbiturate Derivatives as Corrosion Inhibitors

Kadhim A. Ali[1], Mohanad M. Kareem[2] and Hamida I. Salman[1]

[1]Department of Chemistry, College of Education for Pure Sciences, University of Karbala, Karbala, Iraq.

[2]Department of Chemistry, College of Science, University of Babylon, P.O. Box 51002, Hilla, Iraq.

***E-mail:** Mustafa97162@gmail.com **;** Sci.mohanad.mousa@uobabylon.edu.iq ; Hamida.idan@uokerbala.edu.iq

ARTICLE INFO

Article History
Received:16/10/2023
Accepted:24/11/2023
Available:28/11/2023

Keywords:
Thermodynamic functions, Alloys, Corrosion, Barbiturates, Adsorption isotherm, Potentiometry, cathodic inhibitors.

ABSTRACT

The study's focus is on the use of potentiostat technology to stop the corrosion of mild steel alloys using various barbiturates which are newly prepared compounds. It has been synthesized and described by 13C, FTIR, and 1HNMR techniques at concentrations ranging from 0 to 200 ppm in a 1M sulfuric acid solution at temperatures between 303 and 323 K. Anode and cathode curves (a, c), corrosion current density (Icorr), corrosion potential (Ecorr), and efficiency inhibition ratio (E%) were used in the experiments, and the results were presented.DFT calculations have been performed to understand the nature of the interactions between the inhibitor molecules and the surface of the alloy to be tested.

The influence of temperature and concentration on the effectiveness of inhibition was examined. The prepared compound used as an inhibitor is effective and a good corrosion inhibitor in mild steel alloy under the experimental conditions used, where the highest inhibition efficiency was 85.30% at a rising temperature and increasing inhibitor concentration, according to the results. 200ppm concentration at 323K in temperature. were also examined and talked about. it was found that the adsorption of the two compounds obeys Langmuir, which elaborated the thermodynamic functions of the adsorption operation (ΔSads, ΔHads, ΔGads).

INTRODUCTION

One of the main problems in many manufacturing sectors is metal corrosion, which causes enormous economic losses (Salghi *et al.*, 2017). usage of corrosion. One of the best ways to prevent corrosion on metal surfaces in situations with acidic chemicals is to use inhibitors(Lagrenee *et al.*, 2002). Due to its affordability, usefulness and availability in abundance, mild steel is used extensively across a variety of industries. Acid solutions are typically employed in a variety of industrial operations to remove unwanted rust, scale, etc. As a result, solutions containing corrosive ions are frequently exposed to metallic surfaces. A key issue with these applications is corrosion, Corrosion causes significant losses in the industrial sectors, and the greatest defense against it is the protection procedure. Corrosion inhibitor is regarded as the greatest kind of protection in the business among the different techniques utilized to shield the metal surface from deterioration and destruction(Rani and Basu 2012),(Chigondo and Chigondo 2016).

The fact that organic substances have some impacted elements, such as electronegativity and conjugation, makes them the most effective inhibitors. The adsorption on the surface of the metal is influenced by the physical and chemical characteristics of the molecule, such as size, donor-acceptor atoms, orbital p character, electronic structure, and types of functional groups (Obot and Obi-Egbedi 2008). Organic compounds that contain heterocyclic atoms in their structure, such as (sulfur, nitrogen, phosphorus, and oxygen), whether they are in the ring or in the side chain, or compounds that contain electrons, or effective polar groups (NO2, -SH, -NH2, -OH) which increases its adsorption on the surface of the metal increases the efficiency of its inhibition(Dutta *et al.,* 2017). By adsorbing the inhibitor particles onto the metal's surface, an insulating defense barrier is formed between the metal's surface and the acidic solution, preventing or reducing corrosion(Abd-Alkareem, Salman, and Hassan 2023), and the efficiency of organic inhibitors depends on the chemical composition, the size of the aromatic organic inhibitor, the carbon chain binding chain, the nature and charge of the metal surface of the type of adsorption, the ability of the inhibitor to bind The surface of the metal, the type and number of atoms or groups attached to the molecule (skama and pi), the active groups the inhibitor contains, the type of electrolyte solution(El Mouden *et al.,* 2015).

Organic substances having Schiff's bases an amine in which the nitrogen atom is bonded to an aryl or an alkyl group but not a hydrogen atom. Its general equation is R1R2C = N-R3. Amine is stabilized via the organic interaction with the nitrogen atom possible inhibition(Alnasrawi *et al.,* 2020),(El-Barasi *et al.,* 2023). The main benefit of Schiff Rules is that they are inexpensive starting materials and can be deployed effortlessly. Effective Chef Guidelines Steel corrosion inhibitors for the presence of imine (-C = N-) and electrophilic groups in acidic medium The molecule(Abdel-Gaber *et al.,* 2009),(Gupta *et al.,* 2016).Contains oxygen, nitrogen, and/or sulfur. Barbiturates have a "balance" of lipophilic functionality (5,5'-substituents) and hydrophilic activity (2,4,6-pyrimidinetrione ring structure). Barbiturates' general hydrophilic (polar) or lipophilic (non-polar) nature depends on: - The total size and structure of the two substituents at the 5-position, which is dependent on the number of N-substituents and the pKa of the acidic proton(s) in the pyrimidinetrione ring. in 5 position. Barbiturates, such as phenobarbital, have long been used as anxiolytics and hypnotics and reduce REM sleep time. Today they have been largely replaced by benzodiazepines for these purposes because the latter are less toxic in drug overdose(Sunkara *et al.,* 2004),(Albert Jones 2018),(Whitlock* 1975). Barbiturates can be used as a biological antibacterial. Planar molecules tend to absorb the metal surface better than those having less planar structure, which is influenced by the geometry of molecule structure. It has been discovered that quantum calculations are an effective tool for illuminating the mechanism of corrosion inhibition (Johns 1975),(Liu *et al.,* 2011).

Environmental chemicals with little to no environmental influence are preferred by corrosion prevention systems. According to the available evidence, organic inhibitors work by adhering to metal surfaces and forming protective films. According to the following procedure organic inhibitor molecules replace water molecules at the metal/solution interface to cause the adsorption of those molecules(Chetouani *et al.,* 2003). Carbon steel that is used in petroleum pipelines and building and bridge structures has good mechanical properties however it undergoes corrosion and it needs methods of corrosion protection. (Oũm 1970).In several branches of chemistry, the quantitative structure-activity relationship (QSAR) has attracted a great deal of attention. In the subject of corrosion, the design and development of organic corrosion inhibitors may benefit from the use of density functional

theory (DFT)(Abd-Alkareem, Salman, and Hassan 2023).

To explain the mechanism of inhibiting the effect of heterocyclic organic compounds theoretically, the Density Functional Theory (DFT) method(Khaled 2008),(Awad 2004),(Hegazy e*t al.*, 2013). was used. Quantum Chemical methods have proved very useful in determining molecular structures and explaining electronic structures and reactivity. They have been proven to be a very powerful tool for studying corrosion inhibition mechanisms(Fang and Li 2002).

MATERIALS AND METHODS

Preparation of Organic Inhibitors:

Synthesis of 5-(4-nitrobenzylidene)-2-thioxodihydropyrimidine-4,6(1H,5H)-dione {K1}: Thiobarbituric acid (0.013 mol, 2g), 4-nitrobenzal-aldehyde (0.013 mol, 2.14 g) and sodium acetate (0.013 mol, 1.3 g) was mixed in the mortar. The mixture was finely grounded at room temperature and then the product was dissolved in 10 ml of water, The product was washed with water after that it was dried which afforded a solid yellow product with 71% yield, m.p. decomp.>325 ^{O}C The reaction was monitored by TLC (acetone :chloroform:: 3:2 Rf =0.74). IR (KBr, Vmax ,cm-1) , ,3280 (N-H), 3150 (C-H arom), 3155 (-C=C-H), 1703 (C=O amide), 1604 (C=C alkene), 1620 (C=C arom.) 1535,1344 (NO2), 1405 (C-NO2), 1195 (C-NH), 850 (C=C alkene bend), 738 (C=C arom. Ring bend), ,(Found) % for C_{11} H_7 N_3 O_4 S :C,47.65; H,2.54; N,15.16; O,23.08; S.11.56 .

Synthesis of 4-(4-((4,6-dioxo-2 thioxo tetra hydro pyrimidin-5(2H) yliden) methyl) phenoxy)benzaldehyde (K2): After being cooled to room temperature and rinsed with 1 N HCl and distilled water, a mixture of compound K1 (0.0151 mol, 4 g), 4-nitro benzaldehyde (0.0144, 1.76 g), and K2CO3 (0.0144 mol, 2.13 g) was prepared. The product (K2) with the solid brown color and m.p. >230 oC was produced in 74% yield. TLC was used to observe the reaction (acetone:chloroform 3:2 Rf = 0.62).KBr, Vmax, and cm-1): 3270 (NH), 3150 (C=H arom.), 2720 (C-H alde.), 1704 (C=O alde.) 1641 (C=O amide), 1602 (alkene) 1375 (C=C arom,) 1344 (C-NH) 1050 (Ar-O-Ar). ^{1}H NMR (ppm):): δ 10.56 (2H, NH), 9.79 (H, H-C=O), 8.24 (H, H-C=C), 8.45 (2H, Ar-H),7.98 (6H, Ar-H). 13C NMR (ppm): δ 191.2(C, C-C=O), 165.80 (C, S=C-C), 162.79 (2C, C=O), 156.34 (C, =C-O), 132.56 (2C, C-Ar), 130.49 (C, =C-C=O), 127.80 -116.72 (6C, C-Ar). (found) % for C_{18} H_{12} N_2 O_4 S: C, 61.36; H,3.43 ; N, 7.95; O, 18.16 ; S, 9.11.

Synthesis of 5-(4-(4-(((4 chlorophenyl) imino)methyl) phenoxy) benzylidene)-2-thioxo dihydropyrimidine-4,6(1H,5H)-dione (K_2D_1): A mixture compound **K_2** (0.0042 mol, 2g) in 10ml acetic acid and added p-chloroaniline (0.0042, 0.9g). and three drops of icy acetic acid were heated at 80 ^{o}C with reflex and stirred for 2 h then it remained cool until a precipitate formed after that it was recrystallized with ethanol was weighed with filter paper. The solid brown colour product (K_2D_1) in 62% yield and m.p.>300 ^{o}C. Shown this in **diagram 1**, was obtained the reaction was monitored by TLC (acetone: chloroform 3:2, R_f = 0.53). 3383 (N-H),) 2940 (C-H SP^2) 3100 (C=H arom.), 1675 (C=O amide),1573 (C=N) 1440 (C=S), 1344 (C-NH) ^{1} H NMR (ppm): δ 13.53 (H, NH), 10.8 (H, NH), 8.80 (H, H-C=N), 8.46 (H, C=CH-), 8.27 (d 2H, Ar-H),8.10-7.40 (4H, Ar-H) 7.29-6.55 (6H, Ar-H). ^{13}C NMR (ppm): δ 170.28 (C, S=C-N) 163.2 (2C, C=O) 150.5 (C, C=N) 139.43 (C, =C-O) 134.7 (C, =C-N) 130.6 (C, C-Cl), 128.8 (C, =C-CH) 125.9 (2C, C-Ar) 117.3 (4C, C-Ar). (found) % for $C_{24}H_{16}ClN_3O_3S$, C, 62.41; H, 3.49; Cl, 7.57; N,9.10; O, 10.39; S, 6.94

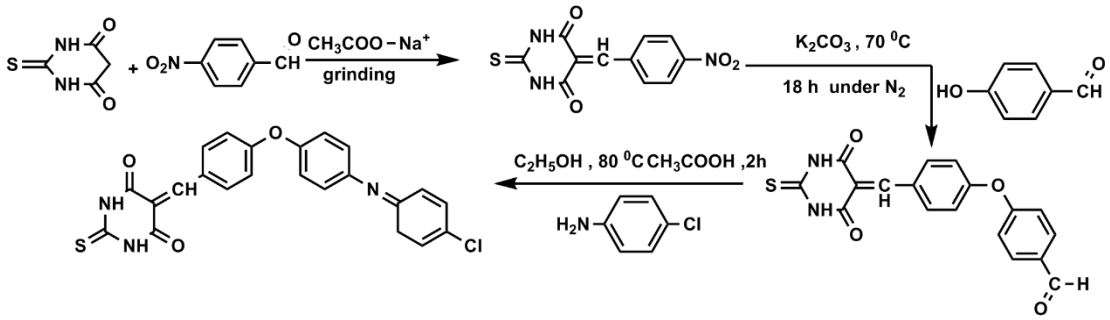

Diagram -1- synthesis of 5-(4-(4-(((4 chlorophenyl) imino)methyl) phenoxy) benzylidene)-2-thioxo dihydropyrimidine-4,6(1H,5H)-dione.

Preparation of Carbon Steel Specimens:

The samples were made by cutting a carbon steel column into cylinders with a diameter of (2.5 cm) and a height of (3 mm). The samples' chemical makeup was identified. Aside from Fe, test samples contained 0.179% C, 0.141% Si, 0.652% Mn, 0.0082% P, and 0.028% S. Other test samples included 0.0545% Cr, 0.0039% Mo, 0.0478% Ni, 0.0105% Al, and 0.224% Cu. Then, mechanical polishing and smoothing operations were carried out utilizing fine polishing equipment and sanding boards with varied grits (80-2500). Each specimen should be washed with 100% ethanol and stored in the dryer until use after polishing the surface and a paste that resembles glass(Abdulridha *et al.*, 2020).

Prepare the Solution:

The solution to be tested is prepared with 1M of H2SO4 by diluting it with 98% sulfuric acid solution with distilled water. Then we prepared a solution of the compound used for inhibition with different concentrations starting (0.005, 0.02, 0., 0.) by dissolving in 1 ml of DMSO and weighing certain quantities to prepare the inhibitors, then they are dissolved in the acid solution and then supplemented with 1000 water.

Measurements of the Potentiodynamic Polarization:

The polarization of the electric potential is calculated through a three-electrode electrochemical cell made of Pyrex glass attached to a potential static. The working electrode in which the alloy is placed, the calomel electrode (SCE Ag / AgCl) measures the saturator, and the auxiliary electrode is composed of platinum. The three electrodes are immersed in a container containing the prepared solution, and they are tested for a period of 30m to obtain open circuit measurements (OCP) in their steady state in a voltage range of (-972 - 50 mv) In it, the electrode stops the counter, after which it is turned on to calculate the electrical measurements of both the E_{corr} and I_{corr} from Through the linear polarization Tafel method of the Bc, Ba curves. The inhibition efficiency[E%] is calculated through the following equation (1)(Bedair *et al.*, 2017).

$$E\% = \frac{Icorr - Iinh}{Icorr} \times 100 \quad \ldots\ldots (1)$$

E% is the inhibition efficiency ratio, I_{corr} is the corrosion current density without the inhibitor and I_{inh} is the current density with the inhibitor.

Quantum Chemical Calculations (DFT):

In order to calculate the most crucial parameters, such as EHOMO, ELUMO, energy gap (E), and parameters that influence the interaction between the prepared inhibitor molecules and the exterior of the material or alloy to be tested on, quantum chemical calculations using density functional theory have been recorded in B3LYP/6-31++G(d, p) level with Gaussian 09W software, which has been linked to GaussView5.0. Since our investigations are conducted in conditions that contain acidity, parameters have been hypothetically recorded for the produced compounds in the liquid phase (1 M H2SO4 in water solvation system over the checkpoint files). The energy levels for the lowest vacant orbit (ELUMO), the highest occupied molecular orbit (EHOMO), and the energy

gap (E) between them will all be determined. Since our studies happen in media, parameters have been theoretically collected for the produced compounds in the liquid phase (1 M H2SO4 in water solvation system over the checkpoint files). Acidity The lowest empty orbit (ELUMO) and the highest occupied orbit (EHOMO) will have their energy levels determined, and the difference between them, or what is known as the energy gap (E), is found in equation (2). The ionization potential energy and electron affinity (A, the negative of ELUMO), are found given by Koopman's theorem (Sastri and Perumareddi 1997).

$\Delta E = EHOMO - ELUMO$…… (2)

$I = -cc$……. (3)

$A = -E_{Lomo}$ …… (4)

The chemical potential and chemical hardness were computed using equations (5) and (6) and the highest occupied E_{Homo} and lowest unoccupied molecular orbitals E_{Lomo}, respectively, in accordance with Koopman's theory. Chemical hardness is a measure of an atom's resistance to charge transfer(Pearson 1988).

$$\text{Chemical Potential} = \mu = -\left(\frac{I+A}{2}\right) = \left(\frac{EHomo+ELomo}{2}\right) \ldots. (5)$$

$$\text{Chemical Hardness} = \eta = \left(\frac{I-A}{2}\right) = \frac{EHomo-ELomo}{2} \ldots\ldots (6)$$

The energy decrease between the donor and acceptor atoms is expressed by the electricity index (ω), which is to the equation (7):

$$\text{Electricity index} = (\omega) = \frac{\mu 2}{2\eta} \ldots\ldots (7)$$

Electronegativity (χ) which represents the ability of molecules to pull an electron towards them, has been calculated as in the equation (8):

$$\text{Electronegativity} = \chi = \left(\frac{I+A}{2}\right) = \left(\frac{EHomo+ELomo}{2}\right) \ldots \ldots (8)$$

RESULTS AND DISCUSSION

Synthesis:

The geometrical optimization findings of [K2D1] Figure (1) parameters show that the data from the FT-IR, 1H NMR, and 13C NMR are similar. The carbonyl group in the aldehyde K2 was bound to the nitrogen atom of the main amine by Schiff base and resulting from the interaction of the N atom in the primary amine with the carbonyl group in the aldehyde or ketone, forming an isomethine group. This interaction between LOMO and HOMO then caused the electron transfer of the responsive species. Because they develop quickly and are stable, aromatic chemicals were chosen. a molecule is more likely to transfer an electron than under the observed circumstances. Indicators of By counting the HOMO's energy (EHOMO), the thermodynamic functions, internal energy, enthalpy, and free compression energy all agreed on their respective positions This is shown in Table (1).

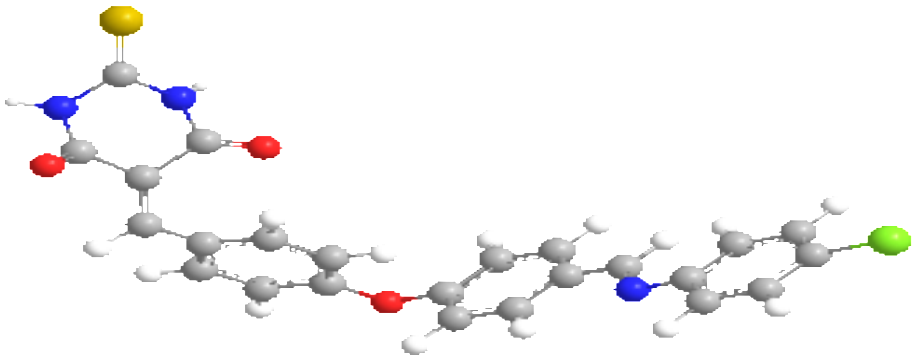

Fig. 1: Optimized geometry for K_2D_1 at the B3LYP/6-31G basis set.

Table 1:Calculation of thermodynamic functions of K_2D_1 , K_2D_4 and K_2D5 BY B3LYP.

Molecules	E KCal/Mol	H (Hartree /Particle)	S Cal/Mol-Kelvin	G Hartree
K_2D_1	134.694	0.215592	161.794	0.138719

Biological Activity:

Antibacterial:

By conducting the test, it was found that the prepared compounds (K2D1, have antibacterial activities Picture 1. The examination was carried out using the agar disc diffusion method(Kareem et al. 2021). Both positive and negative bacteria, such as Staphylococcus aureus, are successfully eliminated. (DMSO) was used. Each of these bacteria was produced in bacterial suspensions at a concentration of 0.5-0.65. It showed a good antibody due to its structure that interacts with the cell wall of the bacteria that were examined(Sangthong et al. 2011). This is shown in the Table (2).

Table 2: Anti-bacterial activity for prepared compounds 1mg/mL concentration.

Comp. s	Gram +ve (Staphylococcus aureus)(mm)	Gram –ve (E-coli) (mm
K_2D_1	**10**	**20**

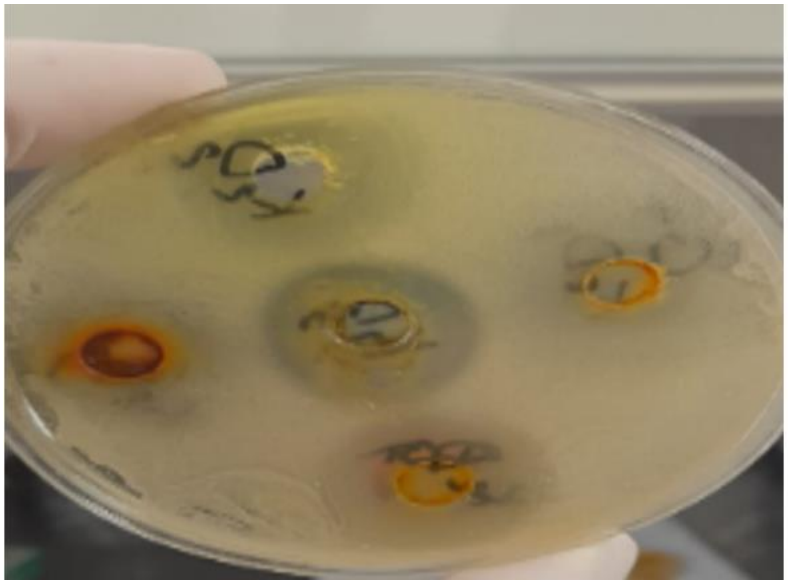

Pic. 1: Anti-bacterial activity of compounds

Table.3 The percentages of the components of the prepared vehicles by CHNS .

COMP.	Calculated %				Found Value %			
	C	**H**	**N**	**S**	**C**	**H**	**N**	**S**
K_2	**61.35**	**3.40**	**7.94**	**9.22**	**60.05**	**3.11**	**7.42**	**8.86**
K_2D_1	**62.34**	**3.46**	**9.09**	**7.03**	**61.43**	**3.21**	**8.89**	**6.55**

Electrochemical Method:

The following Figures (1-3), show the electrochemical analysis of Tafel curves (effective polarization) to find out the effect and efficiency of the prepared inhibitor (as an inhibitor of the corrosion process for a

selected sample of steel in a 1M H2SO4 solution with several concentrations of the prepared compound (K2D1) (0-200) at temperatures from (303 – 323K) and demonstrates the measured electrochemical characteristics, such the corrosion potential (Ecorr), corrosion current (Icorr), anodic and cathodic(βc) Tafel slopes, inhibition efficiency (Ƞ%), and surface coverage (Ɵ). It was found that by adding the inhibitor, the current density increases at a constant concentration and with an increase in temperature, while the current density decreases with an increase in the concentration at a constant temperature. With the increase in temperature, the corrosion process increases, and thus the inhibition efficiency increases. It turned out that the highest efficiency obtained from the experiments was at a concentration of 200 parts of a million at a temperature of 323K(Salman and Manshad 2019).

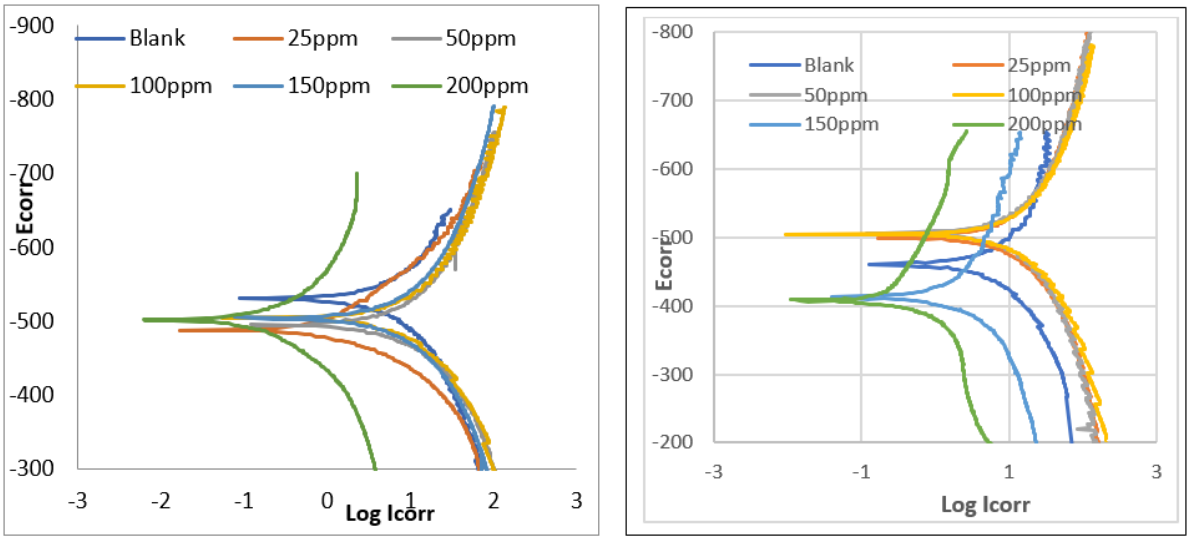

Fig. 1. Polarization curves for the carbon steel corrosion without and with different K_2D_1 concentrations at 313 K.

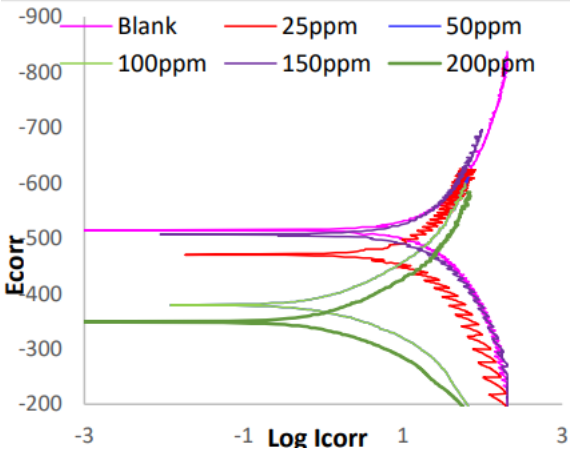

Fig. 2: Polarization curves for the carbon steel corrosion without and with different K_2D_1 concentrations at 313 K

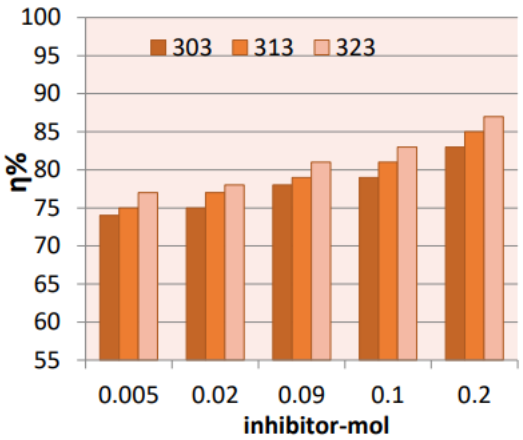

Fig. 3: The impact of temp. variation on the effectiveness of K2D3 inhibition various does.

Adsorption Effect:

When the inhibitor was added, a protective layer was formed for corrosion and protection from the acidic medium on the surface of the alloy resulting from the adsorption process and through adsorption isotherms. It shows us the interaction between the environment and the metal(Hassan and

Hadi 2015). Conducting the test in a thermal range (303 - 323) K by the two types of chemical and physical adsorption and determines the adsorption mechanism by the known Frumkin, Temkin, and Langmuir adsorption equations. The adsorption in our interaction was found to be consistent with the Lanckmuir relationship, and the constants (Kads) were extracted on the basis of Lanckmuir equation (9). We show this in Figure (4). the relationship between the adsorption of the prepared inhibitor with the temperature in the acidic solution and extract the value of free energy (ΔGads) for adsorption from equation (10) and then illustrate it by drawing between Log kads values against 1 / T Figure (5) according to equation (11) to calculate the enthalpy reaction ΔHads, and through the values of ΔGads and ΔHads, the entropy values ΔSads for this process are found from equation (12)(Halambek, Cindrić, and Grassino 2020). The θ: is the amount of surface coverage, C_{inh}: inhibitor concentration, T: temperature, R: constant for gases and The number 55.5 represents the molar concentration of water. the results obtained show that the free energy has negative values, and this indicates that adsorption in this case occurs automatically, while the positive enthalpy values indicate that the particles adsorbed on the test alloy are endothermic. As for the entropy, its positive value indicates randomness. the system (Dehdab et al. 2016),(Kosari et al. 2014).

$$\frac{Cinh}{\theta} = \frac{1}{Kads} + Cinh \quad (9)$$

$$\Delta Gads = - RT \, Ln \, (55.5 \, kads) \quad (10)$$

$$Log \, Kads. = (- \frac{\Delta Hads}{2.303 \, R \, T}) + C_{con} \quad (11)$$

$$\Delta Gads = \Delta Hads - \Delta gads \quad (12)$$

$$\Theta = \eta_p\% / 100 \quad (13).$$

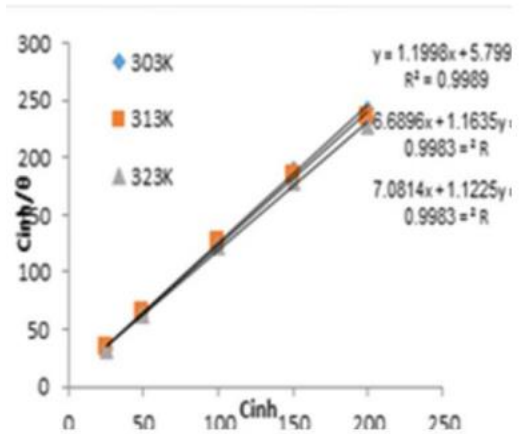

Fig.4: K2D3 adsorption in 1M H2SO4 with a temperature range of (303-333) K according to the Langmuir equation

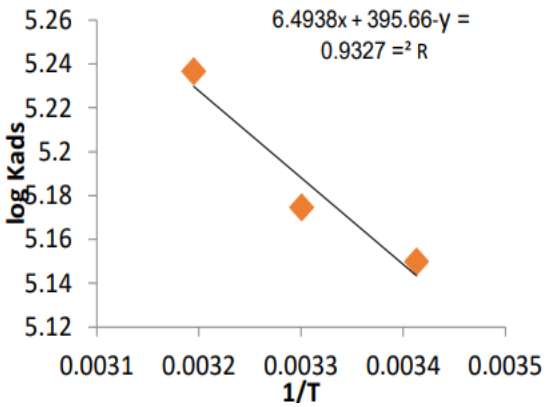

Fig. 5: A Correlation between log Kads vs. 1/T for mild steel corrosion at temp. from (303-323) K and various K_2D_3 conc. In 1M H_2SO_4.

Corrosion Kinetics Study:

It is clear that the temperature has an effect on the corrosion process and on the speed and kinetics of corrosion so it is studied and calculated to obtain information about its effect on the rate of corrosion and through the Arrhenius equation (14) logI_{corr} = log *A*-Ea/2.303RT Where corrosion: corrosion current density, A: Arrhenius constant, Ea: activation energy, R: the gas constant, T: temperature (Abboud *et al.*, 2012). Figure (6), shows the relationship between Log icorr versus 1/T for the corrosion of the alloy in acidic media with the presence or absence of the inhibitor. Also, the activation energy was calculated from the slope of the drawn relationship and Log A, and it was calculated from the intersection of the drawn lines, and through the calculations that we extracted, the enthalpy is calculated ΔH* for the activation energy, randomness or entropy ΔS* and the free compressive energy ΔG* through the

following relationship (Amin *et al.*, 2011).

$$I_{corr} = \frac{RT}{Nh}\, e^{\frac{\Delta s*}{R}}\, e^{\frac{(-\Delta H*)}{RT}} \quad \ldots\ldots\ldots\ldots\ldots\ldots\ldots\ldots (15)$$

$$\Delta G* = \Delta H* - T\Delta S* \ldots\ldots\ldots\ldots\ldots\ldots\ldots (16)$$

Where N: Avogadro's number, h: is Plank's constant" This can be seen in the form () the linear relationship between the Log icon / T versus 1 /T, slopes (ΔH*/2.303R) and intercepts (Log R/N h +ΔS*/2.303R). Table (5), shows values Ea, A, ΔH*, ΔS*, ΔG*. The table () of the kinetic parameters data confirms that the activation energy increased with the presence of the organic inhibitor that we prepared compared to the absence of the inhibitor (K_2D_1) in relation to the enthalpy ΔH* (Sliem et al. 2019). The movement of the reacting molecules on the alloy, which is transformed into adsorbent molecules and the entropy increases in the presence of the inhibitor. The free energy values indicated that the process was spontaneous(El Ouali et al. 2010),(Ahmed, Ali, and Khadom 2019).

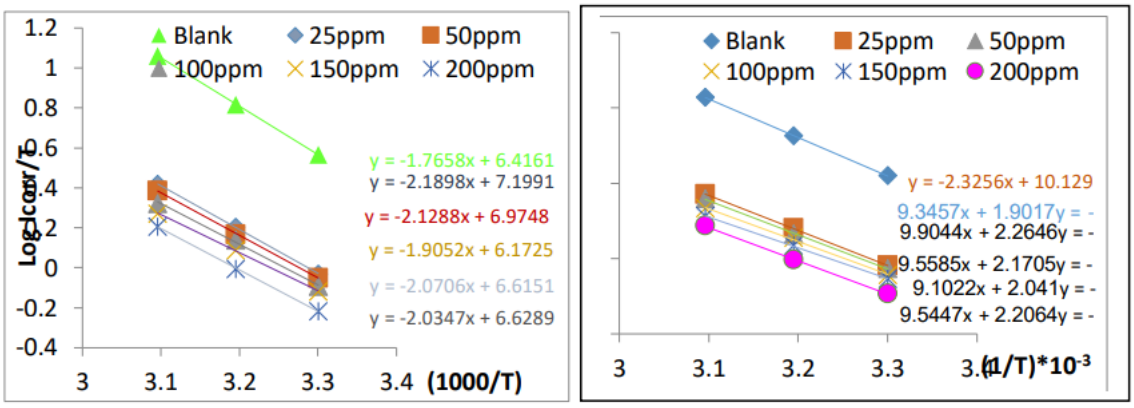

Fig. 6: shows the Arrhenius ratio for the corrosion of carbon steel in 1MH2SO4 at temperatures between 303 and 333 K. B: The correlation between log icorr/T and 1/T both with and without AS across the temperature from 303-333 K**.**

Table (5). The activation parameters for carbon steel corrosion at 303–333 K in the presence and absence of different K2D2 concentrations.

CAS (mM)	Ea kJ mol−1	ΔH* kJ mol−1	−ΔS* J mol^{-1} K^{-1} ∗ 10^{-2}
25	44.5285	41.9284	59.7338
50	43.3606	40.7604	64.0285
100	41.5588	38.9586	70.6515
150	39.0793	36.4791	79.3902
200	42.2462	39.6460	70.9157
Blank	36.4121	33.8100	74.7260

Quantum Chemical Calculations (DFT):

To ascertain the reality of the interactions between the particles of the prepared compounds and the surface of the alloy, DFT tests were conducted, as the composition of the particles affects the physical and chemical properties of the particles. For the optimized Shapes for the upper filled orbitals (HOMO) and the lower unoccupied (LUMO), where the results showed the electronic density distribution of (HOMO) that the compound has the ability to give electrons to the adsorbent centers in the surface of the alloy distributed in general, especially the π-orbitals of the cyclic compounds that contain Heterogeneous atoms. As for the density distribution of (LUMO)(Tan et al. 2018) its ability to absorb electrons from the surface of the alloy to the adsorbent centers. Because it contains a strong cloud group and has the highest ability to give and receive electrons, where this

feature has the tendency of molecules to give and receive in relation to energy levels (HOMO). This is shown in Table (7), the highest ability to give an electron and (LUMO) levels, the highest ability to accept it whereas in the second molecule containing an electron-donating group, this difference was less pronounced. Energy Gab (E(HOMO-LUMO). ΔE = EHOMO−ELUMO), which is a higher inhibition efficiency, i.e. the formation of a protective layer through the adsorption of inhibitor molecules on the surface of the alloy. and this indicates that the protonal form has a good effect on the inhibition process in acidic media, and thus it achieved High inhibition efficiency according to Table (3)'s findings, the molecules are arranged according to their hardness, which is consistent with the previous sentence's description of the energy gap. This is because, according to the law of chemical hardness's (ɳ (ev)) Table (8) definition, the arithmetic rate of the difference between the ionization potential and the electronic affinity determines how hard the molecules are. Along with the type of compensated aggregates and the ability of electronic withdrawal and donation to induce (Jennane *et al.,* 2019)**.**

Table 7: Ehomo and elomo of k_2d_1 by basis set 6-31g at b3lyp

Molecular	**E_{HOMO} (ev)**	**E_{LOMO} (ev)**
K_2D_1	**-0.20284**	**-0.17883**

Table 8: Guantum parameters for, k_2d_3 molecules by basis set 6-31g at b3lyp

Molecules	**ɳ (ev)**	**IP (ev)**	**EA (ev)**	**Energy gap (ev)**
K_2D_1	0.012005	0.20284	0.17883	0.02401

CONCLUSIONS

The new barbiturate derivative was identified by FTIR, HNMR and 13C techniques. It was experimented as an inhibitor for carbon steel alloys in H2SO4 1M solution with good results. Through electrochemical experiments, it was discovered that the produced compound effectively inhibits the corrosion impact on the alloy's surface. The inhibition efficiency raised with increasing the concentration and temperature rise, and vice versa. According to the Langmuir adsorption equation, molecules are adsorbed on the alloy surface. DFT studies revealed that there are several molecular adsorption sites and that these sites have molecular orbitals with energy gaps and levels.

REFERENCES

Abboud, Y et al. 2012. "5-Naphthylazo-8-Hydroxyquinoline (5NA8HQ) as a Novel Corrosion Inhibitor for Mild Steel in Hydrochloric Acid Solution." *Research on Chemical Intermediates* 38: 1591–1607.

Abd-Alkareem, Saja Ahmed, Hamida Idan Salman, and Sajid Hassan. 2023. "Polar Extract of Echhornia Crassipes Used as Corrosion Inhibitor in 1M HCL." In *AIP Conference Proceedings*, AIP Publishing.

Abdel-Gaber, A M, M S Masoud, E A Khalil, and E E Shehata. 2009. "Electrochemical Study on the Effect of Schiff Base and Its Cobalt Complex on the Acid Corrosion of Steel." *Corrosion Science* 51(12): 3021–24.

Abdulridha, Ali Ahmed et al. 2020. "Corrosion Inhibition of Carbon Steel in 1 M H2SO4 Using New Azo Schiff Compound: Electrochemical, Gravimetric, Adsorption, Surface and DFT Studies." *Journal of Molecular Liquids* 315.

Ahmed, Salima K, Wassan B Ali, and Anees A Khadom. 2019. "Synthesis and

Investigations of Heterocyclic Compounds as Corrosion Inhibitors for Mild Steel in Hydrochloric Acid." *International Journal of Industrial Chemistry* 10: 159–73.

Albert Jones, David. 2018. "Assisted Dying and Suicide Prevention." *Journal of Disability & Religion* 22(3): 298–316.

Alnasrawi, Taha H, Shatha Abd_Alameer Jawad, Hamida Edan Salman, and Mohammed Ridha Al-Haideri. 2020. "Synthesis, Characterization and Study of Schiff Base Ligand Type N2 and Metal Complexes with Di Valence Nickel, Copper and Zinc." *International Journal of Pharmaceutical Research* 1: 1246–51.

Amin, Mohammed A et al. 2011. "Monitoring Corrosion and Corrosion Control of Iron in HCl by Non-Ionic Surfactants of the TRITON-X Series–Part II. Temperature Effect, Activation Energies and Thermodynamics of Adsorption." *Corrosion science* 53(2): 540–48.

Awad, Mohamed K. 2004. "Semiempirical Investigation of the Inhibition Efficiency of Thiourea Derivatives as Corrosion Inhibitors." *Journal of Electroanalytical Chemistry* 567(2): 219–25.

Bedair, M A, M M B El-Sabbah, A S Fouda, and H M Elaryian. 2017. "Synthesis, Electrochemical and Quantum Chemical Studies of Some Prepared Surfactants Based on Azodye and Schiff Base as Corrosion Inhibitors for Steel in Acid Medium." *Corrosion science* 128: 54–72.

Chetouani, A et al. 2003. "Corrosion Inhibitors for Iron in Hydrochloride Acid Solution by Newly Synthesised Pyridazine Derivatives." *Corrosion Science* 45(8): 1675–84.

Chigondo, Marko, and Fidelis Chigondo. 2016. "Recent Natural Corrosion Inhibitors for Mild Steel: An Overview." *Journal of Chemistry* 2016.

Dehdab, Maryam, Zahra Yavari, Mahdieh Darijani, and Afshar Bargahi. 2016. "The Inhibition of Carbon-Steel Corrosion in Seawater by Streptomycin and Tetracycline Antibiotics: An Experimental and Theoretical Study." *Desalination* 400: 7–17.

Dutta, Alokdut et al. 2017. "Effect of Substitution on Corrosion Inhibition Properties of 2-(Substituted Phenyl) Benzimidazole Derivatives on Mild Steel in 1 M HCl Solution: A Combined Experimental and Theoretical Approach." *Corrosion Science* 123: 256–66.

El-Barasi, N M et al. 2023. "Synthesis, Characterization, Theoretical Study and Biological Evaluation of Schiff Base and Their La (III), Ce (IV) and UO2 (II) Complexes." *Bulletin of the Chemical Society of Ethiopia* 37(2): 335–46.

Fang, Jian, and Jie Li. 2002. "Quantum Chemistry Study on the Relationship between Molecular Structure and Corrosion Inhibition Efficiency of Amides." *Journal of Molecular Structure: Theochem* 593(1–3): 179–85.

Gupta, Neeraj Kumar, Chandrabhan Verma, M A Quraishi, and A K Mukherjee. 2016. "Schiff's Bases Derived from l-Lysine and Aromatic Aldehydes as Green Corrosion Inhibitors for Mild Steel: Experimental and Theoretical Studies." *Journal of Molecular Liquids* 215: 47–57.

Halambek, Jasna, Ines Cindrić, and Antonela Ninčević Grassino. 2020. "Evaluation of Pectin Isolated from Tomato Peel Waste as Natural Tin Corrosion Inhibitor in Sodium Chloride/Acetic Acid Solution." *Carbohydrate polymers* 234: 115940.

Hassan, S A, and A K Hadi. 2015. "Sudan III as Corrosion Inhıbıtor for Carbon Steel St37− 2 in H2SO4 Solutıons."

International Journal of Scientific Research, 6(7): 5445–53.

Hegazy, M A, A M Badawi, S S Abd El Rehim, and W M Kamel. 2013. "Corrosion Inhibition of Carbon Steel Using Novel N-(2-(2-Mercaptoacetoxy) Ethyl)-N, N-Dimethyl Dodecan-1-Aminium Bromide during Acid Pickling." *Corrosion Science* 69: 110–22.

Jennane, Jamila et al. 2019. "Influence of Sodium Gluconate and Cetyltrimethylammonium Bromide on the Corrosion Behavior of Duplex (α-β) Brass in Sulfuric Acid Solution." *Materials Chemistry and Physics* 227: 200–210.

Johns, M W. 1975. "Sleep and Hypnotic Drugs." *Drugs* 9: 448–78.

Kareem, Mohanad Mousa, Nour Abdalrazzak, Saadon Aowda, and Nagham Mahmood Aljamali. 2021. "Synthesis, Characterization and Biological Activity Study for New Hybrid Polymers by Grafting 1, 3, 4-Triazole and 1, 2, 4-Oxadiazle Moieties onto Polyvinyl Chloride." *Egyptian Journal of Chemistry* 64(3): 1273–83.

Khaled, K F. 2008. "Adsorption and Inhibitive Properties of a New Synthesized Guanidine Derivative on Corrosion of Copper in 0.5 M H2SO4." *Applied Surface Science* 255(5): 1811–18.

Kosari, Ali et al. 2014. "Electrochemical and Quantum Chemical Assessment of Two Organic Compounds from Pyridine Derivatives as Corrosion Inhibitors for Mild Steel in HCl Solution under Stagnant Condition and Hydrodynamic Flow." *Corrosion Science* 78: 138–50.

Lagrenee, M et al. 2002. "Study of the Mechanism and Inhibiting Efficiency of 3, 5-Bis (4-Methylthiophenyl)-4H-1, 2, 4-Triazole on Mild Steel Corrosion in Acidic Media." *Corrosion Science* 44(3): 573–88.

Liu, Pengju et al. 2011. "Electrochemical and Quantum Chemical Studies of 5-Substituted Tetrazoles as Corrosion Inhibitors for Copper in Aerated 0.5 MH 2 SO 4 Solution." *Materials Sciences and Applications* 2(09): 1268.

El Mouden, O Id et al. 2015. "Inhibitive Action of Capparis Spinosa Extract on the Corrosion of Carbon Steel in an Aqueous Medium of Hydrochloric Acid." *Journal of Mineral Metal and Material Engineering* 1: 1–7.

Obot, I B, and N O Obi-Egbedi. 2008. "Inhibitory Effect and Adsorption Characteristics of 2, 3-Diaminonaphthalene at Aluminum/Hydrochloric Acid Interface: Experimental and Theoretical Study." *Surface Review and Letters* 15(06): 903–10.

El Ouali, I et al. 2010. "Thermodynamic Characterisation of Steel Corrosion in HCl in the Presence of 2-Phenylthieno (3, 2-b) Quinoxaline." *Journal of Materials and Environmental Science*, 1(1): 1–8.

OÕM, J. 1970. "Bockris, AKN Reddy, Modern Electrochemistry Vol. 1."

Pearson, Ralph G. 1988. "Absolute Electronegativity and Hardness: Application to Inorganic Chemistry." *Inorganic chemistry* 27(4): 734–40.

Rani, B E, and Bharathi Bai J Basu. 2012. "Green Inhibitors for Corrosion Protection of Metals and Alloys: An Overview." *International Journal of corrosion* 2012.

Salghi, R et al. 2017. "6-Phenylpyridazin-3 (2H) One as New Corrosion Inhibitor for C38 Steel in 1 M HCl." *International Journal of Electrochemical Science* 12(4): 3309–22.

Salman, Hamida Edan, and Mj Manshad. 2019. "Methyl Violet Dye as Corrosion Inhibitor for Carbon Steel in Acidic Medium." *Journal of*

Global Pharma Technology 12(01).

Sangthong, Supranee et al. 2011. "Synthesis of Rotenoid Derivatives with Cytotoxic and Topoisomerase II Inhibitory Activities." *Bioorganic & medicinal chemistry letters* 21(16): 4813–18.

Sastri, V S, and J R Perumareddi. 1997. "Molecular Orbital Theoretical Studies of Some Organic Corrosion Inhibitors." *Corrosion* 53(08).

Sliem, Mostafa H et al. 2019. "AEO7 Surfactant as an Eco-Friendly Corrosion Inhibitor for Carbon Steel in HCl Solution." *Scientific reports* 9(1): 2319.

Sunkara, Gangadhar et al. 2004. "Systemic and Ocular Pharmacokinetics of N-4-benzoylaminophenylsulfonylglycine (BAPSG), a Novel Aldose Reductase Inhibitor." *Journal of pharmacy and pharmacology* 56(3): 351–58.

Tan, Bochuan et al. 2018. "A Combined Experimental and Theoretical Study of the Inhibition Effect of Three Disulfide-Based Flavouring Agents for Copper Corrosion in 0.5 M Sulfuric Acid." *Journal of colloid and interface science* 526: 268–80.

WHITLOCK*, F A. 1975. "Suicide in Brisbane, 1956 to 1973: The Drug-death Epidemic." *Medical Journal of Australia* 1(24): 737.